Exchange-correlation effects in the monoclinic to tetragonal phase stabilization of yttrium-doped ZrO_2: A first-principles approach

Davide Sangalli and Alberto Debernardi
MDM Lab-IMM-CNR via C. Olivetti, 2, IT-20864 Agrate Brianza (MB), Italy
(Received 4 November 2011; revised manuscript received 15 December 2011; published 27 December 2011)

We describe, within an *ab initio* approach, the stabilization of the tetragonal phase versus the monoclinic one in yttrium-doped zirconia. The process is believed to be influenced from different mechanisms. Indeed, we show that there is a delicate balance between the change in electrostatic and kinetic energy and exchange-correlation effects. In the tetragonal phase, the perturbation induced by doping is better screened at the price of sacrificing correlation energy. Our work opens the opportunity to use the same approach to predict the tetragonal phase stabilization of materials such as zirconia or hafnia, with different and less characterized dopants.

DOI: 10.1103/PhysRevB.84.214113 PACS number(s): 64.70.K−, 71.15.Mb, 81.05.Je, 81.30.Bx

I. INTRODUCTION

Zirconia (ZrO_2) is a hard and usually colorless material with a wide range of technological applications.[1] Being corrosion resistant, it is used as a dental material, and because of its low cost, durability, and close visual likeness to diamond, it is widely used to synthesize artificial gems. It is used as a thermal barrier in coating engines due to its high resistance. The addition of cations (as, for example, Y^{3+}) induces the generation of oxygen vacancies for charge compensation, which makes it useful as oxygen sensor. Moreover, zirconia is a high dielectric constant (high-κ) material with potential applications in the microelectronics. Finally, very recently, transition-metal-doped zirconia has been predicted to be a dilute magnetic semiconductor (DMS) with high Curie temperature T_c with potential applications in the field of spintronics,[2] while pure and doped ZrO_2 has been proposed as a candidate material for resistive switching memories devices[3,4] (ReRAM) exploiting the high-vacancy mobility of the system.

Pure ZrO_2 exhibits at ambient pressure three polymorphisms. The monoclinic (M) phase is stable at low temperature and is the less symmetric structure with the Zr^{4+} ions exhibiting sevenfold coordination. Between 1440 and 2640 K, the tetragonal (T) phase with eightfold-coordinated Zr^{4+} ions is stable. Finally, above 2640 K, until melting temperature (≈3000 K), the most symmetric cubic (C) phase is stabilized.[5,6] The only difference between the (C) and the (T) phases is a distortion of the oxygen sublattice with a spontaneous symmetry breaking. The (T) and (C) phases are more used in technological applications and both the (T)/(C) structures and the (T) → (C) doping-induced phase transition (DIPT) have been well characterized in the literature both from the theoretical and the experimental points of view,[5,7–16] with Y^{3+} ions the most used and studied dopants.

On the other hand, the (M) → (T) DIPT is much less characterized, especially from the theoretical point of view. It presents a volume change of about 3–4% that causes extensive cracking in the material. This behavior destroys the mechanical properties of fabricated components and makes pure zirconia useless for structural or mechanical applications. Moreover, the (T) phase is metastable in pure and lightly doped ZrO_2 over a very long time; a growth sample of doped zirconia must be annealed in order to check if the reached tetragonal phase is stable or metastable. Hence, a better understanding of the (M) → (T) DIPT is desirable. In this paper, we address the problem from a first-principles perspective and, in particular, we show that the DIPT is a balance of the mean-field (MF) description (i.e., kinetic plus electrostatic: $H = T + V^{\text{ext}} + V_H[\rho]$) with exchange-correlation effects, which can not be captured by simplified models.

II. FIRST-PRINCIPLES DESCRIPTION

A. Computational details

We work within density functional theory[19,20] (DFT) in the generalized gradient approximation[21] (GGA) with ultrasoft pseudopotentials.[22,23] Both for yttrium and zirconium, the pseudopotentials include semicore electrons and nonlocal core correction. The QUANTUM ESPRESSO (Ref. 24) package is used to solve the Kohn-Sham[20] (KS) equations for a supercell with 96 atoms (down to 92 when oxygen vacancies are considered). We checked that a cutoff of 35 Ry for the wave functions and 400 Ry for the augmentation charge, and a k-point grid $2 \times 2 \times 2$ are needed in order to have the energy difference between the tetragonal and the monoclinic phases converged to up to 5.0×10^{-4} eV per ZrO_2 molecular unit (m.u.), where the energy difference is of the order of 0.1–0.01 eV/m.u.

As a starting point, we relaxed atomic positions and structure of pure ZrO_2 with 12 atoms in the unit cell of the (T) and (M) phases. The (C) phase is unstable and is not considered at zero doping.[25] The results, reported in Tables I and II, are in good agreement with experimental data and previous theoretical works within the DFT error (≈1-2%).

We correctly find that the (M) phase is favored with an energy difference $\Delta E_{M-T} = 0.109$ (eV/mol) in agreement with previous works [0.063 (eV/mol) (Ref. 8) and 0.144 (eV/mol) (Ref. 6)]; the experimental estimation is 0.063 (eV/mol).[27]

B. Yttria-stabilized zirconia

The (T) and the (C) phases of zirconia can be stabilized with yttria (Y_2O_3) doping, with a phase diagram for yttria-stabilized zirconia (YSZ), which has been extensively characterized experimentally. Also, the (T) and (C) phases of Y-doped

TABLE I. Theoretical and experimental cell parameters of ZrO_2 in the monoclinic and the tetragonal phases.

This work		Theory		Experiment	
		(M) ZrO_2			
		Ref. 17	Ref. 8	Ref. 14	Ref. 18
a (Å)	5.18	5.05		5.15	5.15
b/a	1.011	1.027		1.012	1.012
c/a	1.037	1.028		1.023	1.032
β	99°10′	99°5′		99°14′	99°14′
		(T) ZrO_2			
a (Å)	5.11	5.02	5.03		5.07
c/a	1.030	1.014	1.017	1.026	1.018

zirconia have been studied within a theoretical approach in a number of works,[8–10] while no systematic study of the Y-doped (M) phase or of the (M) → (T) DIPT has been reported in the literature.

Y doping is known to induce oxygen vacancies. We show in Fig. 1 how the Kohn-Sham (KS) density of states changes if vacancies are present both in pure and doped ZrO_2 crystals at low doping.[28] Moreover, we compute the energy the system gains producing vacancies (see the caption of Fig. 1 for more details) for different doping concentrations. A correct modeling of the material must consider the possible relative positions of the dopants (as substitutional defects) and the vacancies. We found that the relative position of Y atoms among themselves play a minor role, in agreement with the other works,[9] and in our system, we kept these as far as possible to mimic uniform doping. Instead, the position of vacancies with respect to Y atoms or to other vacancies influences significantly the total energy of the system. Stapper *et al.*[8] reported that, in the cubic system, isolated vacancies tend to be next nearest neighbor (NNN) to Y atoms with an energy gain of $\Delta E_c \approx 0.34$ eV per vacancy against the nearest-neighbor (NN) configuration in a supercell with 1 Y atom and 1 vacancy. This result is confirmed also by Ostanin *et al.*[9] in a supercell with 2 Y atoms and 1 vacancy with $\Delta E_c \approx 0.3$ eV between the two configurations ($O\text{-}Y_1$,$O\text{-}Y_2$) = (NN,NNNN) and ($O\text{-}Y_1$,$O\text{-}Y_2$) = (NNN,NNN) in favor of the second in the (C) phase and $\Delta E_t \approx 0.2$ eV in the (T) phase. Also, in this work, we found $\Delta E_t \approx 0.12$ eV, considering 1 vacancy and 2 Y atoms.

In the (M) phase, two nonequivalent oxygen atoms exist, one with coordination 3 and another with coordination 4 and, accordingly, there are four possible configurations. We found that the case (NN, NNNN)$x3$ favored of 0.21, 0.36, and 0.80 eV against (NNN, NNN)$x3$, (NNN, NNN)$x4$ and (NN, NNNN)$x4$, respectively; here, the labels $x3$ and $x4$ refer to the coordination that would have the vacant oxygen. To the best of our knowledge, no results have been reported in the literature about the position of vacancies in the (M) phase.

The most favored configuration, for both the (T) and the (M) phases, is represented in Fig. 2, together with the forces acting on each atom in the initial geometry of pure ZrO_2. The Y ions are not attracted by the oxygen vacancies and indeed in the (M) phase they are pushed away from the vacancy. Hence, both the analysis of the energetically favored configuration and the internal relaxation of the ions do not follow the intuitive scheme of charged defects with the vacancies a $+2e$ and the Y ion a -1 charged site, suggesting that exchange-correlation effects play a role in the stabilization mechanism.

Also, the relative vacancy-vacancy orientation and position is in contrast with an electrostatic-based model. In the (C)/(T) phase, while Stapper *et al.*[8] based their calculation on the assumption that oxygen vacancies should remain as far as possible, Ostanin *et al.*[9] results suggest that oxygen vacancies tend to couple along the [111] direction with a single Zr ion in-between, thus, at a relative distance of about ≈4.47 Å. Also, experimental x-ray data[12] seem to support this idea. No data about the orientation of oxygen vacancies in the (M) phase are present in the literature.

By changing the relative position of divacancy complex in our model (i.e., two vacancy at $x = 12.50\%$), we found differences in total energy of $\Delta E_{\text{tot}} \approx 1.1$ eV (per divacancy). The oscillations in the mean field, i.e., the sum of the kinetic[29] and electrostatic energies, and the exchange-correlation (xc) component of the energy are much more pronounced, with $\Delta E_{\text{xc}} \approx 8.2$ eV and $\Delta E_{\text{MF}} \approx 7.2$ eV. We will discuss this more in detail in the next section. Our results are, in some aspects, different from those suggested by the two cited works. Indeed, we found that, while vacancies do not repel, the configuration suggested as most favorable for the (T) structure by Ostanin *et al.*[9] is not the lowest in energy. Indeed, surprisingly, the latter comes out to be unstable with one of the two vacancies, which changes position if we let the system relax (Fig. 3). This last result suggests that, in the presence of vacancies, oxygen atoms can move with (nearly) no potential barrier to

TABLE II. Theoretical and experimental internal structural parameters of ZrO_2 in the Wyckoff (Ref. 18) notation. For the tetragonal structure, the only free parameter is the z coordinate of the oxygen atoms (0.0, 0.5, 0.25 − d_z).

	This work	Theory	Experiment	
		(M) ZrO_2		
		Ref. 8	Ref. 14	
Zr	(0.276,0.044,0.210)	(0.277,0.043,0.210)	(0.275,0.040,0.208)	
O_I	(0.065,0.327,0.350)	(0.064,0.324,0.352)	(0.070,0.332,0.345)	
O_{II}	(0.451,0.757,0.475)	(0.450,0.756,0.479)	(0.450,0.757,0.479)	
		(T) ZrO_2		
			Ref. 13	Ref. 26
d_z	0.057	0.044	0.057	0.042

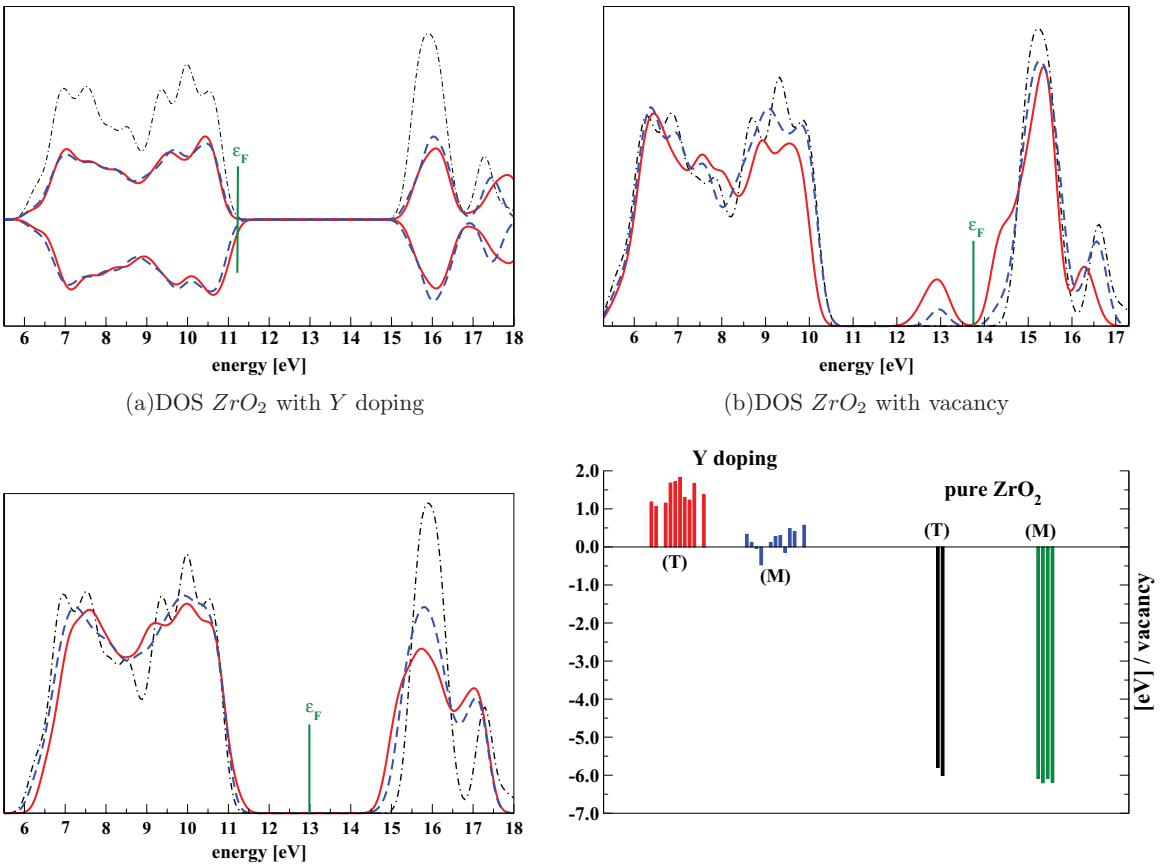

FIG. 1. (Color online) Kohn-Sham density of states for (a) yttrium-doped zirconia ($Zr_{1-x}O_2Y_x$), (b) zirconia with oxygen vacancies ($ZrO_{2-y}V_y$), and (c) zirconia with one vacancy each and two yttrium atoms ($Zr_{1-x}O_{2-y}Y_xV_y$) in the tetragonal phase. The DOS are at $x = 0.25$ and $y = 0.125$ (red continuous line) and $x = 0.125$ and $y = 0.0625$ (orange dashed line); the DOS of pure ZrO_2 (thinner black dotted-dashed line) is also shown. The system doped with yttrium gains energy when vacancies are created, releasing oxygen molecules (d). Here, $E_{\text{gain}} = 1/y\{E(Zr_{1-x}O_2Y_x) - [E(Zr_{1-x}O_{2-y}Y_xV_y) + y/2\mu(O_2)]\}$, with $x = 2y$ for the "Y-doping" case (on the left) and $x = 0$ for pure ZrO_2 (on the right). The creation of vacancies is instead highly unfavored in the undoped system.

overcome. This is a theoretical evidence that YSZ is a good ionic conductor. Indeed, this property is important for many applications and has been investigated in other works.[30]

We also considered some cases at atomic doping concentrations of $x = 18.75\%$ and one test case at $x = 25.00\%$. Both for $x = 12.50\%$ and 18.75%, there is a huge number of possible relative positions of the oxygens and we did not try to systematically explore which is the best configuration. At $x = 12.25\%$, the best found configuration has two vacancies aligned in the xy plane. A simple explanation of this fact could be provided considering the axial anisotropy of the dielectric constant (κ) of the (T) phase. The components $\kappa_{xx} = \kappa_{yy}$ are larger than the κ_{zz}, thus providing a more effective screening of charged oxygen vacancies placed along the xy plane. However, we did not find this to be the sole mechanism, as some of the other configurations with the vacancies aligned in the xy plane have higher energy than some configurations with the vacancies aligned, for example, in the xz plane.

To conclude this section, the behavior of the oxygen vacancies presents some differences, and some similarities, between the two phases of zirconia. A key important difference, however, is that the formation of vacancies is more favored in the (T) phase than in the (M) phase, as one can see from Fig. 1(d). This fact indeed implies that Y_2O_3 doping tends to stabilize the (T) phase.

C. Theoretical stabilization: xc energy and vacancies

The configuration explored allows us to model the (M)→(T) DIPT as a function of the yttria doping. In Fig. 4, we see that the energy difference between the (T) and the (M) phases decreases, increasing the doping concentration. This is a clear signature that we are correctly describing the DIPT. However, the stabilization of the (T) phase happens, after a linear fit of our data, at higher doping concentration (≈14%) than the experimental value (≈7%).[15] The main error is due to an overestimation of the zero-doping energy difference of 0.056 eV/m.u. [$E_{\text{exp}} \approx 0.063$ eV/m.u. (Ref. 27), while $E_{\text{DFT}} \approx 0.109$ eV/m.u.]. Indeed, it is reasonable to assume that the trend of the energy difference is better computed than its absolute value and, accordingly, assuming a constant "zero-doping error" not influenced by the Y concentration we can subtract it (the zero energy in Fig. 4 shifts from the black line to the blue line) obtaining $x_{\text{DIPT}} \approx 7.5\%$, which

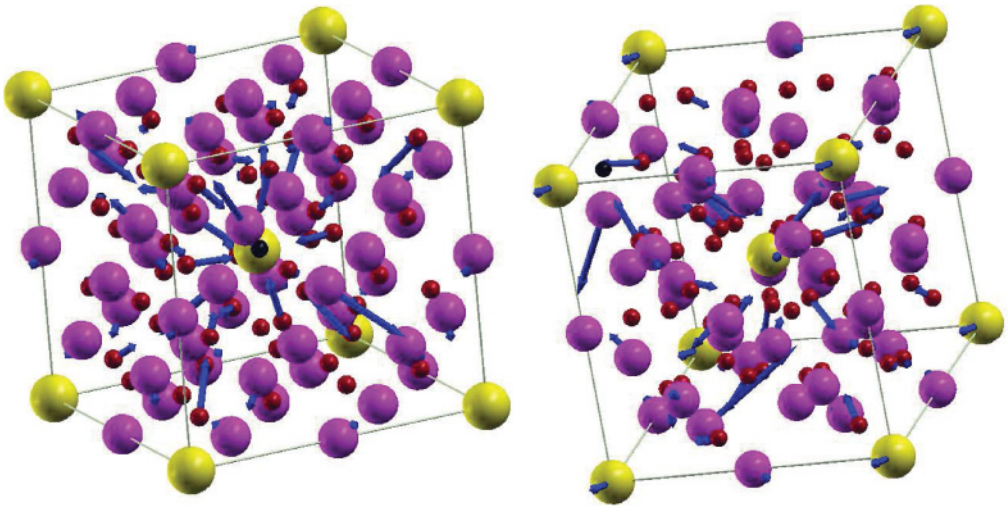

(a) Tetragonal (b) Monoclinic

FIG. 2. (Color online) Tetragonal (a) and monoclinic (b) structures of $Zr_{(1-2x)}Y_{2x}O_{(2-x)}V_x$, with the most stable configuration at $x = 0.031\,25$. The forces acting on the ions in the "starting geometry," i.e., with the atoms placed at the coordinates of the relaxed ZrO_2 system, are represented with blue arrows. In the tetragonal structure, the oxygen atoms (O, small red spheres) closer to the oxygen vacancy (V represented as a small black sphere in the figure) move toward it of $\approx$0.3$-$0.5 Å, while the zirconium atom's [Zr, big dark (magenta) sphere] next nearest neighbor moves away from it of $\approx$0.1$-$0.2 Å from the "starting geometry." The yttrium atom [Y, biggest light (yellow) sphere] is almost fixed. The behavior is similar in the monoclinic structure, although the vacancy has just three nearest neighbors here, one of which is a yttrium atom. The yttrium atom moves away from the vacancy, suggesting that a charged-defects interaction model based on electrostatic is not correct and that exchange-correlation effects play a major role.

is in excellent agreement with the experimental value. Similar results are obtained if one considers, instead of the linear fit, the energy difference between the two best configurations (orange dashed line in Fig. 4).

For the pure ZrO_2, we have also computed the contribution to the Helmholtz free energy due to thermal excitations of phonons. We found that the difference in the thermal contribution is negligible at room temperature, while the difference of the zero-point phonon energy between the two phases is $\approx$0.005 eV/m.u., with a small effect on the value of x_{DIPT} (in Fig. 4, this amounts to the shift of the zero from the dashed to the continuous line).

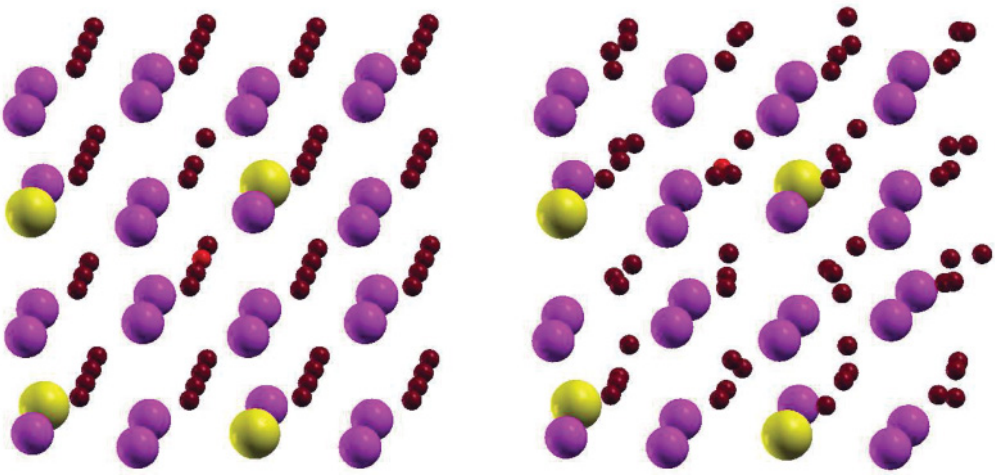

(a) Starting geometry (b) Relaxed geometry

FIG. 3. (Color online) Starting (a) and final relaxed geometry (b) of the $Zr_{1-x}O_{2-x/2}Y_xV_{x/2}$ system with $x = 12.5\%$. O atoms are dark (red) small spheres, Zr atoms are big dark spheres (magenta), and Y atoms are biggest light spheres (yellow). The oxygen that changes position is a small light (light red) sphere. Before relaxation, the two vacancies are aligned along the [111] direction at a distance of 8.45 bohr; they can be detected as (in the figure) the oxygens are aligned in groups of four atoms everywhere except where a vacancy exists. After the relaxation, two vacancies are aligned along the [101] direction at a distance of $\approx$6.2 bohr (this is the distance that the missing oxygens would have at the geometry of pure ZrO_2).

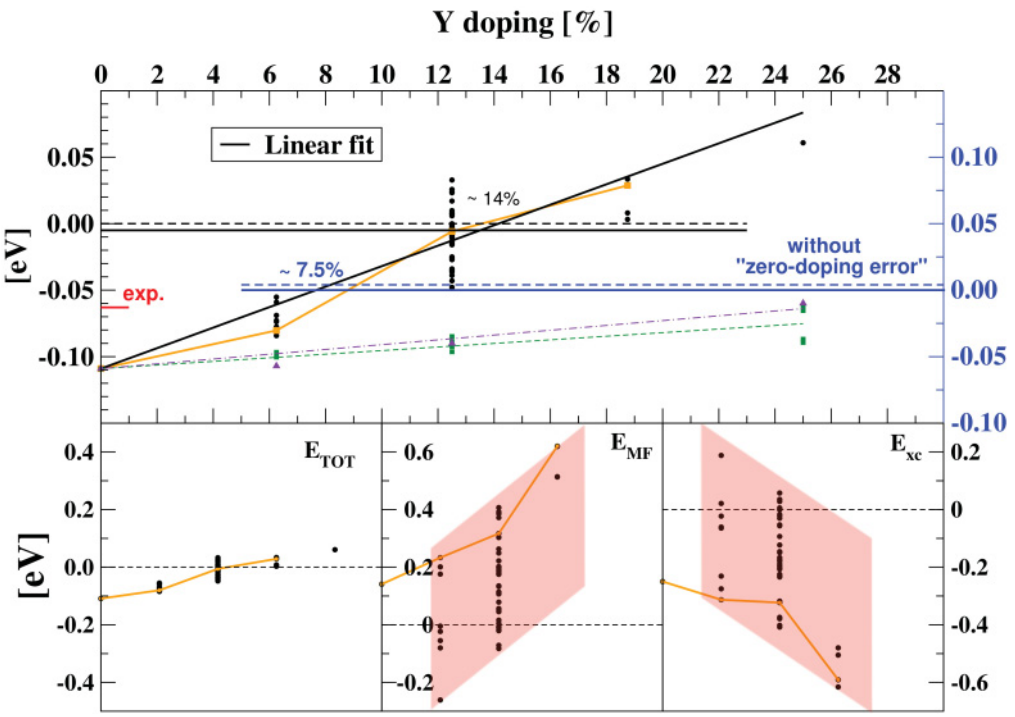

FIG. 4. (Color online) The difference in total energy per molecular unit (upper panel) between the monoclinic and the tetragonal phases decreases, increasing the Y_2O_3 doping (black circles). The result is not simply the sum of the effect induced by Y doping without vacancies (violet triangles, dotted-dashed line for the linear fit) and oxygen vacancies without yttrium (green squares, dashed line for the linear fit). When no yttrium is present, the value of the x coordinate is chosen so that the number of vacancies for the Y_2O_3 doping case is equal to the number of vacancies for the oxygen vacancies' only case. In the bottom panels, the variations in the total energy as a function of the configurations are compared with the variations in the mean field and exchange-correlation energy. The pink shadowed areas are there as guide for the eyes, to highlight the trend of the two energy components.

It is interesting to compare how the mean-field energy $E_{\mathrm{MF}}[\rho] = T[\rho] + V^{\mathrm{ext}} + V_H[\rho]$ and the exchange-correlation energy $E_{\mathrm{xc}}[\rho]$ change considering different configurations. In Fig. 4, bottom panels, we see that the two components oscillate about 10 times more than the total energy as a function of the chosen atomic configuration. The mean-field energy, in pure ZrO_2, is lower in the (T) phase (Fig. 4, central bottom panel); that is, if the xc energy is neglected, the (T) phase is thermodynamically the most stable. The inclusion of Y doping and oxygen vacancies enhances this aspect as, on average, $d(\Delta E_{\mathrm{MF}})/dx > 0$, with x the atomic doping content and $\Delta E_{\mathrm{MF}} = E_{\mathrm{MF}}^{(M)} - E_{\mathrm{MF}}^{(T)}$. This is likely because the tetragonal phase, which has a higher dielectric constant, better screens the electrostatic perturbation $V_{\mathrm{doping}}^{\mathrm{ext}}$ induced by the doping.[31]

In order to have a picture of the screening effect, we have defined (see Fig. 5 and caption) the polarization charge, which is the difference in the electronic density between the pure and the doped systems. In Fig. 5, we see that the main perturbation is induced by the oxygen vacancies. The screening mechanism, however, is very efficient and accordingly the value of the polarization charge is sensibly different from zero only on the atoms NN to the vacancies.

The xc energy in pure ZrO_2 instead is lower in the (M) phase and, on average, $d\Delta E_{\mathrm{xc}}/dx < 0$. To understand this point, we consider the perturbations induced in the electronic part of the Hamiltonian of pure ZrO_2, that is, $V^{\mathrm{pert}} = V_{\mathrm{doping}}^{\mathrm{ext}} + V_{\mathrm{ions}}^{\mathrm{ind}}$, where $V_{\mathrm{ions}}^{\mathrm{ind}}$ is the additional perturbation generated from the dislocation of the atoms. V^{pert} has the shape of a random potential in a perfect periodic system, which tends to destroy the collective behavior of the electron gas and thus electrons lose correlation. This is not an "onsite" correlation but rather a "ranged" correlation energy, and so we expect that GGA can better describe this effect than LDA. While $V_{\mathrm{doping}}^{\mathrm{ext}}$ is similar for the two phases, i.e., we are considering the same kind of doping, the $V_{\mathrm{ions}}^{\mathrm{ind}}$ term is greater in the (T) phase due to its higher screening (see Ref. 31). Accordingly, the xc energy is more penalized, that is, $dE_{\mathrm{xc}}^{(M)}/dx < dE_{\mathrm{xc}}^{(T)}/dx$. This explains $d\Delta E_{\mathrm{xc}}/dx < 0$ and thus we can infer that in the screening process, electrons lose xc energy.

The emerging picture is that the $(M) \rightarrow (T)$ DIPT is a balance between different mechanisms with a key role played by vacancies,[32] although the role of yttrium atoms is not only to induce vacancies (see Fig. 4 and caption).

III. CONCLUSIONS

The phase transition of zirconia induced with yttria doping is very well known experimentally and, indeed, yttria-stabilized zirconia is commonly used in many applications. Our results show that an *ab initio* approach is able to correctly describe this mechanism, with a predicted phase transition at a doping concentration of $\approx$7.5%, in good agreement with experimental data. This result confirms the

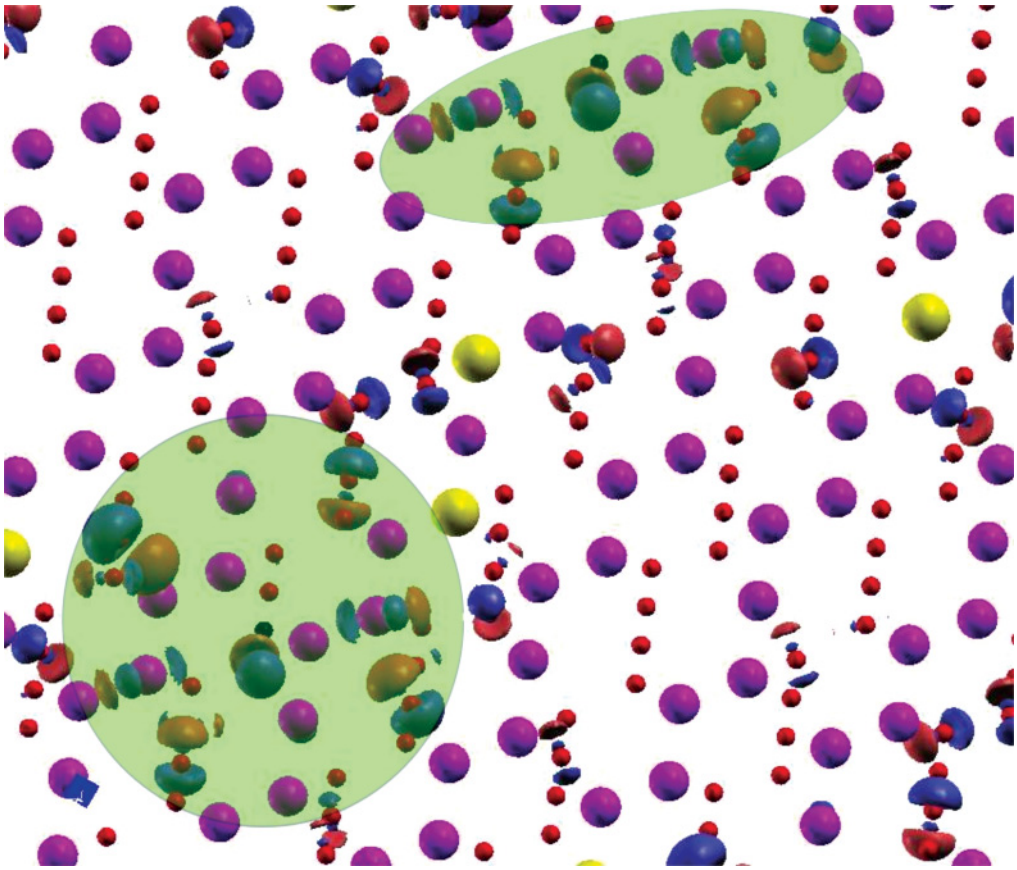

FIG. 5. (Color online) 3D plot of the polarization charge, in the tetragonal phase, defined as $\rho_{\mathrm{pol}} = [32\rho(\mathrm{Zr}_{0.94}\mathrm{O}_{1.97}\mathrm{Y}_{0.06}\mathrm{V}_{0.03}) + \rho(\mathrm{O})] - 32\rho(\mathrm{ZrO}_2)$: isosurfaces for $\rho_{\mathrm{pol}} = \pm\rho_0$ are represented, with the positive ones in red (lighter), the negatives in blue (darker). Oxygen atoms are the small spheres (red), zirconium atoms the dark big spheres (magenta), and yttrium atoms the light biggest spheres (yellow). The (green) shadowed regions highlight the regions around an oxygen vacancy (small black sphere in center of the region), where ρ_{pol} is different from zero.

opportunity to predict the effect of other less characterized kinds of doping, which could be of potential interest for new applications as, for example, doping with magnetic materials.[2]

Moreover, within density functional theory, we can explore how physical properties of the system are influenced by doping. As an example, we considered how different components of the energy changes and, in particular, the behavior of the exchange-correlation energy. We showed that oxygen defects play a major role in the phase transition and how the perturbation induced by oxygen vacancies to the system is screened in the high-κ tetragonal phase. The same approach could be used to check the effect of doping on other quantities, which are not easily accessible experimentally; among others, the value of the dielectric constant has a key importance for applications in the field of microelectronics.

Finally, these results, improving our understanding of the phase transition, can also be used to tune the parameters of models for the description of realistic devices based on zirconia, the dimensions of which are still beyond the capabilities of first-principles simulations.

ACKNOWLEDGMENTS

This work was funded by the Cariplo Foundation through the OSEA project (No. 2009-2552). The authors would like to acknowledge G. Onida and the ETSF (Ref. 33) Milan node for the opportunity of running simulations on the "etsfmi cluster." We also acknowledge computational resources provided under the project OSEA by the Consorzio Interuniversitario per le Applicazioni di Supercalcolo Per Universitá e Ricerca (CASPUR).

[1] *Advances in Ceramics*, edited by A. Heurer and L. W. Hobbs (The American Ceramic Society, Westerville, OH, 1981), Vol. 3; *Advances in Ceramics*, edited by A. Heurer and L. W. Hobbs (The American Ceramic Society, Westerville, OH, 1984), Vol. 12.

[2] S. Ostanin, A. Ernst, L. M. Sandratskii, P. Bruno, M. Däne, I. D. Hughes, J. B. Staunton, W. Hergert, I. Mertig, and J. Kudrnovsky, Phys. Rev. Lett. **98**, 016101 (2007).

[3] X. Wu, P. Zhou, J. Li, L. Y. Chen, H. B. Lv, Y. Y. Li, and T. A. Tang, Appl. Phys. Lett. **90**, 183507 (2007).

[4]H. Zhang, B. Gao, B. Sun, G. Chen, L. Zeng, L. Liu, X. Liu, J. Lu, R. Han, J. Kang, and B. Yu, Appl. Phys. Lett. **96**, 123502 (2010).
[5]G.-M. Rignanese, J. Phys.: Condens. Matter **17**, R357 (2005).
[6]J. K. Dewhurst and J. E. Lowther, Phys. Rev. B **57**, 741 (1998).
[7]E. V. Stefanovich, A. L. Shluger, and C. R. A. Catlow, Phys. Rev. B **49**, 11560 (1994).
[8]G. Stapper, M. Bernasconi, N. Nicoloso, and M. Parrinello, Phys. Rev. B **59**, 797 (1999).
[9]S. Ostanin, A. J. Craven, D. W. McComb, D. Vlachos, A. Alavi, A. T. Paxton, and M. W. Finnis, Phys. Rev. B **65**, 224109 (2002).
[10]S. Ostanin, E. Salamatov, A. J. Craven, D. W. McComb, and D. Vlachos, Phys. Rev. B **66**, 132105 (2002).
[11]K. C. Lau and B. Dunlap, J. Phys.: Condens. Matter **21**, 145402 (2009).
[12]J. P. Goff, W. Hayes, S. Hull, M. T. Hutchings, and K. N. Clausen, Phys. Rev. B **59**, 14202 (1999).
[13]P. Aldebert and J. P. Traverse, J. Am. Ceram. Soc. **68**, 34 (1985).
[14]C. J. Howard, R. J. Hill, and B. E. Reichert, Acta Crystallogr., Sect. B: Struct. Sci. **44**, 116 (1988).
[15]D. G. Lamas and N. E. Walsöe De Reca, J. Mater. Sci. **35**, 5563 (2000).
[16]D. R. Clarke and C. G. Levi, Annu. Rev. Mater. Res. **33**, 383 (2003).
[17]H. Jiang, R. I. Gomez-Abal, P. Rinke, and M. Scheffler, Phys. Rev. B **81**, 085119 (2010).
[18]R. W. G. Wyckoff, *Crystal Structure* (Interscience, New York, 1996).
[19]P. Hohenberg and W. Kohn, Phys. Rev. **136**, B864 (1964).
[20]W. Kohn and L. J. Sham, Phys. Rev. **140**, A1133 (1965).
[21]J. P. Perdew, K. Burke, and M. Ernzerhof, Phys. Rev. Lett. **77**, 3865 (1996).
[22]D. Vanderbilt, Phys. Rev. B **41**, 7892(R) (1990).
[23]A. M. Rappe, K. M. Rabe, E. Kaxiras, and J. D. Joannopoulos, Phys. Rev. B **41**, 1227(R) (1990).
[24]P. Giannozzi, S. Baroni, N. Bonini, M. Calandra, R. Car, C. Cavazzoni, D. Ceresoli, G. L. Chiarotti, M. Cococcioni, I. Dabo, A. Dal Corso, S. Fabris, G. Fratesi, S. de Gironcoli, R. Gebauer, U. Gerstmann, C. Gougoussis, A. Kokalj, M. Lazzeri, L. Martin-Samos, N. Marzari, F. Mauri, R. Mazzarello, S. Paolini, A. Pasquarello, L. Paulatto, C. Sbraccia, S. Scandolo, G. Sclauzero, A. P. Seitsonen, A. Smogunov, P. Umari, and R. M. Wentzcovitch, J. Phys.: Condens. Matter **21**, 395502 (2009); [http://www.quantum-espresso.org].
[25]Also, for the doped case, we considered only the (M) and the (T) phases. Indeed, the (C) phase is a special (T) phase with $c/a = 1$ and $d_z = 0$. The description of this phase is included in our work as we let the atoms relax their position and, in a few cases, also the cell parameters.
[26]M. Fukuhara and I. Yamauchi, J. Mater. Sci. **28**, 4681 (1993).
[27]R. J. Ackermann, E. G. Rauh, and C. A. Alexander, High Temp. Sci. **7**, 304 (1975).
[28]Although these are not the physical DOS, in other works (Refs. 17 and 34), it has been shown that for ZrO_2 the main difference with the real DOS amounts in a red-shift of the gap as common within DFT and LDA.
[29]Here, what we consider is the KS kinetic energy.
[30]F. Pietrucci, M. Bernasconi, A. Laio, and M. Parrinello, Phys. Rev. B **78**, 094301 (2008).
[31]Here, we are studying the response of pure ZrO_2 to a static external perturbation $V^{\rm ext}_{\rm doping}$. The self-consistent solution, in the Bohr-Oppenheimer approximation, of the ionic plus the electronic Hamiltonian $H^{I+{\rm el}}_{ZrO_2}[\rho] + V^{\rm ext}_{\rm doping}$ describes the full response of the system to this perturbation. For a comparison, the static dielectric $\epsilon(0)$ constant of pure ZrO_2 can give an insight as to how the system will react to this perturbation to linear order. In the self-consistent solution, the phononic contribution to the dielectric constant $\epsilon_{\rm ph}(0)$ is accounted for by the relaxation of the atomic positions, while the electronic contribution $\epsilon_{\rm el}(0)$ is accounted for by the the solution electronic part of the Hamiltonian $H^{\rm el}_{ZrO_2}[\rho] + V^{\rm ext}_{\rm doping} + V^{\rm ind}_{\rm ions}$. In high-$\kappa$ materials such as zirconia, the contribution from the lattice is dominant. The (T) phase has higher dielectric constant and, accordingly, we expect a greater distortion of the crystal, provided that the linear order behavior is respected to all orders.
[32]Recent experimental results seem to suggest that the (T) phase can be stabilized simply by inducing oxygen vacancies, tailoring the growing conditions of the sample, without the inclusion of other dopants (Ref. 35).
[33][http://www.etsf.it]; [http://www.etsf.eu]; K. Sanderson, Nature (London) **450**, 777 (2007).
[34]M. Grüning, R. Shaltaf, and G.-M. Rignanese, Phys. Rev. B **81**, 035330 (2010).
[35]A. Lamperti, L. Lamagna, G. Congedo, and S. Spiga, J. Electrochem. Soc. **158**, G221 (2011).